Phase Transformations of Individual Ti_3O_5 Nanocrystals Studied by In Situ Electron Microscopy

Yaowei Hu, Hilaire Mba, Matthieu Picher, Céline Mariette, Hiroko Tokoro, Shin-Ichi Ohkoshi, Ritwika Mandal, Maryam Alashoor, Philippe Rabiller, Maciej Lorenc, et al.

▶ **To cite this version:**

Yaowei Hu, Hilaire Mba, Matthieu Picher, Céline Mariette, Hiroko Tokoro, et al.. Phase Transformations of Individual Ti_3O_5 Nanocrystals Studied by In Situ Electron Microscopy. Journal of Physical Chemistry C, 2024, 128 (33), pp.13991-13997. 10.1021/acs.jpcc.4c02685 . hal-04670589

HAL Id: hal-04670589

https://cnrs.hal.science/hal-04670589v1

Submitted on 12 Aug 2024

HAL is a multi-disciplinary open access archive for the deposit and dissemination of scientific research documents, whether they are published or not. The documents may come from teaching and research institutions in France or abroad, or from public or private research centers.

L'archive ouverte pluridisciplinaire **HAL**, est destinée au dépôt et à la diffusion de documents scientifiques de niveau recherche, publiés ou non, émanant des établissements d'enseignement et de recherche français ou étrangers, des laboratoires publics ou privés.

Phase Transformations of Individual Ti_3O_5 Nanocrystals Studied by *In-Situ* Electron Microscopy

Yaowei Hu[1#], Hilaire Mba[1#], Matthieu Picher[1], Hiroko Tokoro[2]*, Shin-ichi Ohkoshi[3], Céline Mariette[4], Ritwika Mandal[5], Maryam Alashoor[5], Philippe Rabiller[5]*, Maciej Lorenc[5], and Florian Banhart[1]*

[1] Institut de Physique et Chimie des Matériaux, UMR 7504, Université de Strasbourg, CNRS, 67034 Strasbourg, France

[2] Department of Materials Science, Institute of Pure and Applied Sciences, University of Tsukuba, Tsukuba 305-8577, Japan

[3] Department of Chemistry, School of Science, The University of Tokyo, Bunkyo-ku, Tokyo 113-0033, Japan

[4] ESRF - The European Synchrotron Facility, 38043 Grenoble, France

[5] Université de Rennes, CNRS, Institut de Physique de Rennes, UMR 6251, 35042 Rennes, France

[#] These authors contributed equally to this work

* tokoro@ims.tsukuba.ac.jp

* philippe.rabiller@univ-rennes.fr

* florian.banhart@ipcms.unistra.fr

Abstract

Phase changes in individual sub-micron crystals of Ti_3O_5 are studied by *in-situ* transmission electron microscopy. An irreversible transition from the stable beta- to the metastable lambda-phase is induced by slow temperature changes in thermal equilibrium or by nanosecond laser pulses. The expansion of the crystals during the phase transformation is measured in real space by imaging and in reciprocal space by electron diffraction. An incomplete or suppressed phase transformation under slow heating indicates that the kinetic barrier for the thermal transformations from the beta- to the lambda-phase and to the high-temperature alpha-phase is higher than in bulk material. On the other hand, a single nanosecond laser pulse at 1064 nm is found to induce a complete transformation from the beta- to the lambda-phase in sub-micron-size crystals of Ti_3O_5. As in previous studies, laser pulses at longer wavelengths (1064 nm) are found to be more appropriate than at shorter wavelength (532 nm) where inter-band transitions and the rupture of bonds occur. Here, the laser pulses lead to a purely thermal switching from the beta- to the lambda-phase.

I. INTRODUCTION

Photoswitchable materials are an important class of quantum materials[1,2] that challenge our understanding of solids and open avenues for next generation technologies. They are rooted in complex interactions between spin, charge, lattice and orbital degrees of freedom, as well as the topological properties of their wave functions. Photoswitchable materials are sensitive to external stimuli such as electromagnetic fields, *e.g.*, laser pulses, pressure, strain or doping, which give access to various phases, making them ideal candidates for a variety of future technological applications.

Trititanium pentoxide (Ti_3O_5) is a highly promising material for applications in long-term heat storage,[3,4] solar steam generation,[5] or optical memories.[6] The switching between different crystallographic phases can be achieved by external stimuli such as temperature, pressure, or short laser pulses. At room temperature, the semiconducting monoclinic β-phase is stable, whereas another monoclinic structure, the metallic λ-phase, is energetically higher and metastable. The lattice parameters of the λ-phase in the *a*- and *b*-direction are by 1% larger and in the *c*-direction by 6.4% larger than in the β-phase. This leads to a considerable volume expansion during the transition from β to λ. At temperatures above 500 K, the orthorhombic α-phase is reported to be stable.[7] Several morphological forms of Ti_3O_5 have been reported such as single crystals,[8] thin films,[9-12] and nanocrystalline pellets[6,13-15]. A unique behavior of nanocrystalline samples reported by Ohkoshi et al.[6] exhibits several interesting and still poorly understood properties such as the bistability between the semiconducting β- and the metallic λ-phase which is of interest for optical switching or heat storage due to the large latent heat in the reversible transition.[3] The photoswitching between the β and λ phase is a fast process and needs short laser pulses.[16-19] Nanosecond laser pulses are particularly useful for studying fast thermal processes. They are shorter than the propagation time of thermal waves through the crystals but not so short that undesired surface ablation or non-uniform heat distribution such as under femtosecond laser pulses occur.

The dynamics of phase transitions triggered by laser excitation has been studied by optical spectroscopy,[16,17] X-ray diffraction (XRD)[18,19] and ultrafast electron diffraction,[20] and are continually debated. Time-resolved powder diffraction with X-ray Free Electron Lasers and synchrotron radiation allowed a quantitative refinement of the structures during transitions at femto- to microsecond time scales. XRD experiments revealed the propagation of a laser-induced phase front starting from the surface of the crystals and moving with sonic speed into the bulk[19]. This process restores mechanical equilibrium and takes place on an ultrafast timescale and precedes the much slower thermal diffusion. The results point to a phase transition triggered by the laser-induced strain wave within a single grain, yet the clear-cut evidence at this level is lacking because data are averaged on much larger spatial scales than the grain size of the nanocrystals[18,21]. Crystal grain dimensions, laser penetration depth, and the range of the phase transformation were similar (around 100 nm), hence impeding the determination of the limiting factor for transition.

All X-ray diffraction measurements of Ti_3O_5 hitherto[6,18,21] have been undertaken by macroscopic techniques, averaging over a large number of Ti_3O_5 crystallites (e.g., compressed in a pellet for X-ray diffraction studies). Although information about the transformation dynamics was obtained, the behavior of individual crystals remained unclear. Electron diffraction as well as lattice imaging in the TEM has already shown to reveal valuable information in the study of phase transformations in individual oxide crystals, e.g., in VO_2.[22] In a recent work, it has been shown that ultrafast electron diffraction of Ti_3O_5 in a TEM is remarkably suited for such a study with high spatial and temporal resolution and allows time-resolved measurements of the lattice parameters of a single crystal lamella.[20]

However, information in real and reciprocal space within single Ti_3O_5 nanocrystals in irreversible phase transitions (i.e., the volume expansion in the transition from β to λ) hasn't been studied yet. This is the subject of the present work where *in-situ* electron microscopy allows imaging and electron diffraction of individual sub-micron crystals either in equilibrium in a large temperature range or under laser pulses where metastable states can be created under non-equilibrium conditions. In addition to electron diffraction, TEM imaging allows to measure the expansion of crystalline grains, here for the first time in real space during the phase transformation between the β- and λ-phase of Ti_3O_5. We show the phase changes in single sub-micron Ti_3O_5 crystals as a function of temperature by TEM and electron diffraction in equilibrium and under nanosecond laser pulses.

2. MATERIALS AND METHODS

The starting materials for the synthesis were nano-samples taken from ball-milled λ-Ti_3O_5 powder. The latter was obtained from calcinating anatase TiO_2 nanoparticles under hydrogen with a flow speed of 0.3 dm^{-3} min^{-1} at 1200°C for 2 hours. After 6 hours ball-milling, the powder contained almost 100% β-Ti_3O_5 crystallites where the size ranges from hundred nanometers to micrometers. The powder was sonicated in ethanol and dispersed on holey carbon grids for electron microscopy studies. A TEM with acceleration voltage of 200 kV and an attached laser system was used (see Sect. 1 of the supporting information). Continuous heating was achieved by a standard TEM heating stage. To facilitate the identification of the respective phases, crystals with sizes of less than 1 µm were searched where a crystallographic zone axis was close to the optical axis of the microscope. The particles were mostly monocrystalline but showed defected zones due to heavy deformation in the ball milling process.[23,24] Since the crystals turned out to be sensitive to electron irradiation, the electron dose was always kept as low as possible to avoid radiation damage. Due to the radiation sensitivity of the crystals, taking diffraction patterns from the same crystals in different zone axis orientations turned out to be challenging. Diffraction patterns were taken with a beam current density of the order 1 mA/cm^2 on the specimen. The maximum electron dose until the crystals showed changes was approximately 10^3 electrons/$Å^2$.

Lattice images of Ti_3O_5 crystals that have already been shown in other work[12] need an elevated local electron dose which turned out to be too high for in-situ lattice imaging of the phase transformation (see Sect. 2 in the supporting information).

In a first set of experiments, the structure of the crystals in equilibrium was studied at different temperatures by using a heating TEM specimen stage. Diffraction patterns of individual nanocrystals were taken at different temperatures to find out under which thermal conditions the transition between the β-, λ-, and α-phase occurs. Since most of the crystals studied here have a diameter in the range 500 nm – 1 µm, the diffraction information stems from the periphery of the particles where the projected thickness is low. In imaging, shape changes (projected onto the image plane) during the phase transformation of the crystals were observed. Since the heating stage did not allow tilting the specimen relative to the electron beam, crystals with an orientation not too far from a low-indexed zone axis were chosen.

In the second set of experiments, the Ti_3O_5 crystals were exposed to nanosecond laser pulses. An electron microscope with an attached laser-optical system for time-resolved measurements[25,26] was used that allows exposure of the specimen to laser pulses during TEM imaging or diffraction. More detailed information about the setup is given in Sect. 1 in the supporting information. In these experiments, a continuous electron beam from a thermal emitter was used. Laser pulses with a duration of 7 ns and wavelengths of 1064 nm or 532 nm were applied. The power of the pulses was adjustable up to approximately 30 mJ/cm^2. This is a more challenging regime for the sample because of the rather high laser power required to promote the permanent phase change[6] as compared to transient switching in the low-power regime.[16,18,20]

Since the β- and λ-phases of Ti_3O_5 have the same monoclinic space group C2/m and only slightly different lattice parameters, the unambiguous determination of the respective phase is difficult with electron diffraction patterns of one single nanocrystal. The identification of the high-temperature α-phase is less problematic because it appears in the orthorhombic phase (space group Cmcm). For indexing the diffraction patterns, we coded a dedicated graphical interface toolkit to perform the indexation of electron diffraction patterns (see Sect. 5 and 6 in the supporting information). It is based on the least square refinement of a 2D grid going through a set of selected observed diffraction peaks. Miller indices corresponding to the two basis vectors (q_1, q_2) of the zero order Laue zone are looked-up in a table, built from a set of cell parameters corresponding to a possible expected phase and within a fixed uncertainty range in both the vector moduli and the angle. Among possible solutions, we choose indexing that minimizes the root mean square deviation between experimental diffraction peaks and nodes of the model lattice. Equivalent domains may be chosen, minimizing the angle between normal vectors of diffraction layers, when indexing different phases for the same sample. This program is particularly suited for measuring small changes of lattice parameters during the phase transformation. The measurement error can thus be reduced to 1% or less. The fit of several diffraction spots in 2D reveals more information about the respective phase of the crystals than

lattice images in real space where only the crystal planes within the resolution limit of the microscope are available.

3. RESULTS AND DISCUSSION

3.1. Transformations during slow heating and cooling of the crystals

In the first set of experiments, the phase transitions of individual crystals were studied during slow temperature ramps. Figure 1 shows a Ti_3O_5 crystal with a diameter of approximately 600 nm during a heating-cooling cycle between 290 K and 623 K together with the experimental and simulated diffraction patterns. The diffraction patterns show phase transformations under both heating and cooling. The diffraction pattern at room temperature before heating (Figure 1d) is in accordance with the β-phase (Figure 1g); at 623 K (Figure 1e) with the α-phase (Figure 1h), and after cooling to room temperature (Figure 1f) with the λ-phase (Figure 1i) of Ti_3O_5. It is apparent that the crystal has undergone the transformation β → α → λ during the temperature cycle and that the metastable λ-phase can be created during heating and successive cooling. A slight rotation of the crystal occurred during both transformations, which can be depicted in the images (according to the simulated diffraction patterns, the rotation angle in the transformations β → α and α → λ are respectively about ~13° and ~19°). This can be attributed to a shape change during the phase transformation, and to a rotation of the sample which is weakly attached to the specimen grid.

From the comparison of the diffraction patterns in Figures 1d and e, it is obvious that some diffraction spots of the β-phase remain at 623 K (arrow in Figure 1h) so that the transformation β → α is incomplete. As a consequence, the phase transformation β → α upon heating to at least 623 K is gradual and only appears in some crystallites. After the final transformation α → λ (Figure 1f), several new diffraction spots appear in addition to those related to the λ-phase. Again, the transformation does not lead to a perfect single crystal as some grains in a different phase or orientation appear. Whereas the initial particle (Figure 1a, d) was a single crystal in a well-defined phase, the phase transformations led to a polycrystal where at least two phases coexist. This is surprising in view of the small size of the crystals and might be due to a high defect concentration after the heavy deformation in the ball milling process. Furthermore, the proximity of surfaces in the small crystals might change the local energy balance between the phases. The appearance of faint segments of rings in diffraction patterns and small dark spots in the images of the crystal, in particular in Figures 1c and 1f, indicates the formation of some crystallites with sizes of approximately 10 nm within the larger crystal. These crystals appear in different orientations, as the bright field images show, or even in different phases and contribute to the diffraction pattern. Their number increases during the transformations, most likely due to stress around the defective regions. However, the analysis of the phase transformation is restricted here to the principal spots

emanating from the larger crystal. A possible indexing of the ring-like features in Figures 1e and 1f is shown in Sect. 7 of the Supporting information.

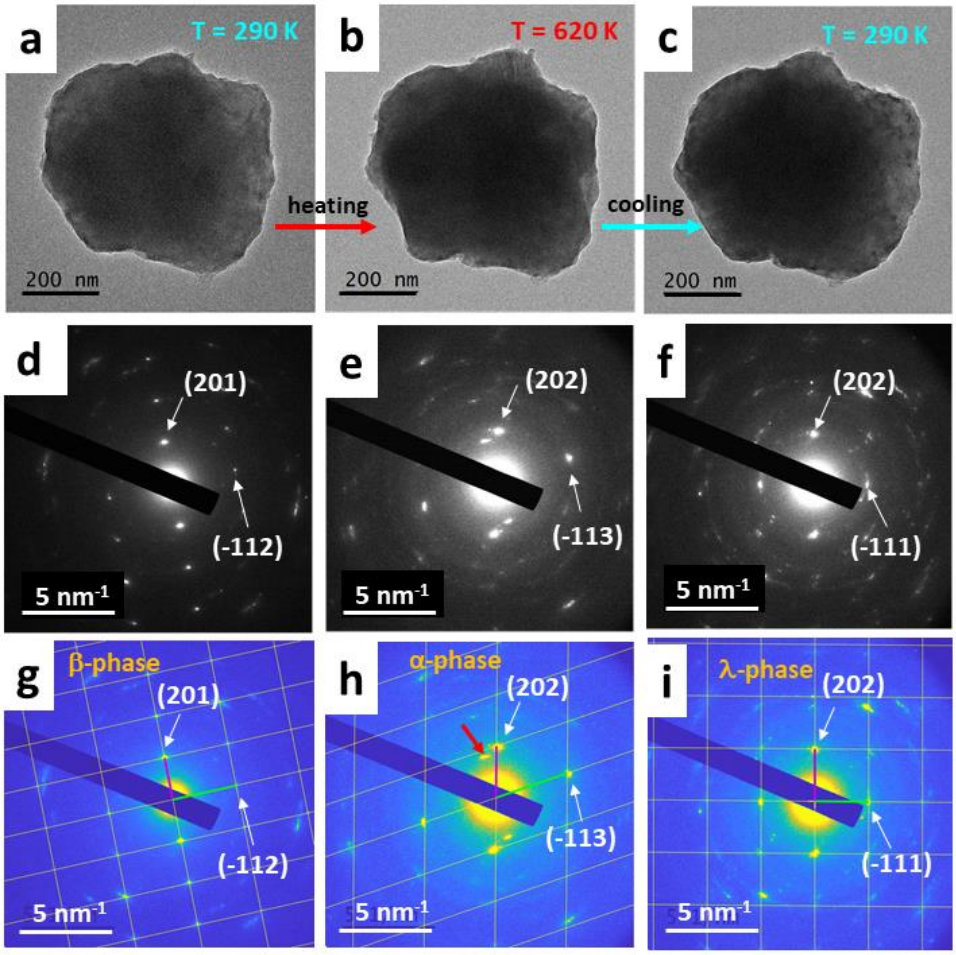

Figure 1. Images, experimental and simulated diffraction patterns of a Ti_3O_5 crystal at different temperatures during a slow heating-cooling cycle. (a, d, g): at room temperature before heating; (b, e, h): at 623 K; (c, f, i): after cooling to room temperature. The diffraction information stems from the projected periphery of the crystals (the thickness in the middle is too high to allow imaging or diffraction at 200 kV).

From the crystallographic data of the three phases[18] (see Sect. 4 in the supporting information), it can be deduced that the lattice parameters of the different axes increase by 1 – 6 % during the transformations β → α and β → λ. The largest expected expansion of the crystal is 6.5 % in the *c*-axis during the transformation β → λ. Due to the changing lattice parameters in the phase transformations, changes of the projected shape of the crystals appear too. However, details depend on the direction of projection onto the image plane.

Figure 2 shows a crystal at room temperature before (Figure 2a) and after (Figure 2b) a heating-cooling cycle where a transformation from the β- to the λ-phase occurred. The expansion is plotted in Figure 2c for different angles relative to the horizontal direction in the image plane. The expansion reaches a maximum along a specific direction (20° in this projection), whereas almost no expansion is visible in the perpendicular direction. Due to the roughness of the surface, some uncertainties of the measurements cannot be excluded, e.g., the difference between 0° (or 180°) and 20° (or between 0° and 160°). The anisotropy of the expansion is confirmed by the analysis of the diffraction patterns in Figure 3. The zero order diffraction layers of the sample shown in Figure 2 was indexed in the two phases β and λ with the two same basis reciprocal vectors (201) and $(\bar{1}10)$ *i.e.* with the lattice direction $[11\bar{2}]$ parallel to the electron beam. (The two reciprocal lattice vectors (201) and $(\bar{1}10)$ correspond to q_1 = 2a* + c* and q_2 = -a* + b*). The relative expansion $\delta L/L$ was also deduced from the changes of basis vectors of the zero order Laue zone diffraction patterns by calculating the transformation of a circle expressed in the β-phase coordinates into the λ-phase coordinates. The result shown in Figure 2d is in good agreement with the value deduced from image inspection, for both the direction (~166°) and magnitude of the maximum elongation (~7%).

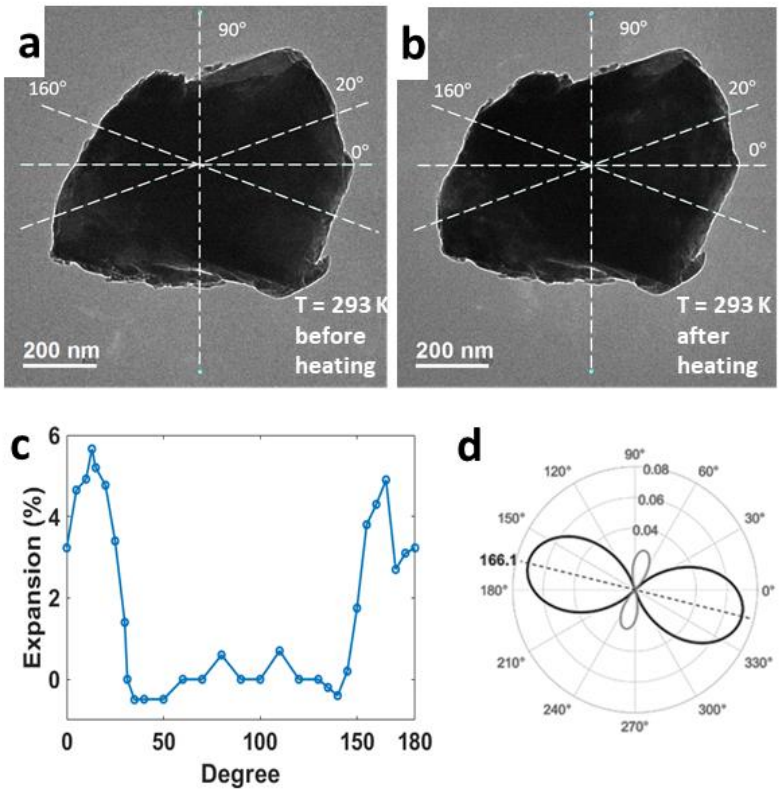

Figure 2. Morphological changes of a Ti_3O_5 crystal before heating (a) and after cooling from 623 K to room temperature (b). The diagram (c) shows the expansion for measurements in

different directions in the image plane (the reference direction 0° is the horizontal). (d) simulation of the relative expansion (thick black line) vs. contraction (thin gray line) as a function of polar angle before and after heating, deduced from the basis vectors of the corresponding zero order Laue zone scattering patterns.

Figure 3a shows the length measurements of the same crystal as in Figure 2 along the direction of maximum expansion (165° in Figure 2) as a function of temperature during a heating-cooling cycle. The corresponding diffraction patterns at four points (marked 1 – 4 along the curve) are shown in Figure 3b. Only minor length changes are measured when the crystal is heated from room temperature to 625 K although the α-phase with larger lattice parameters is expected to prevail above 550 K.[6,7] However, as soon as the crystal is cooled down again, a sudden expansion appears, reaching 5 % when the specimen is cooled down to room temperature. The overall expansion between the β-phase (point 1) and λ-phase (point 4) is in good agreement with the crystallographic data whereas the constant length between points 1 and 2 does not correspond to the expectations for the transformation β → α. The indexing of the respective diffraction patterns (1 – 4) in Figure 3 shows that the β-phase still prevails at 625 K (point 2). Upon cooling, the λ-phase appears suddenly at 550 K (point 3).

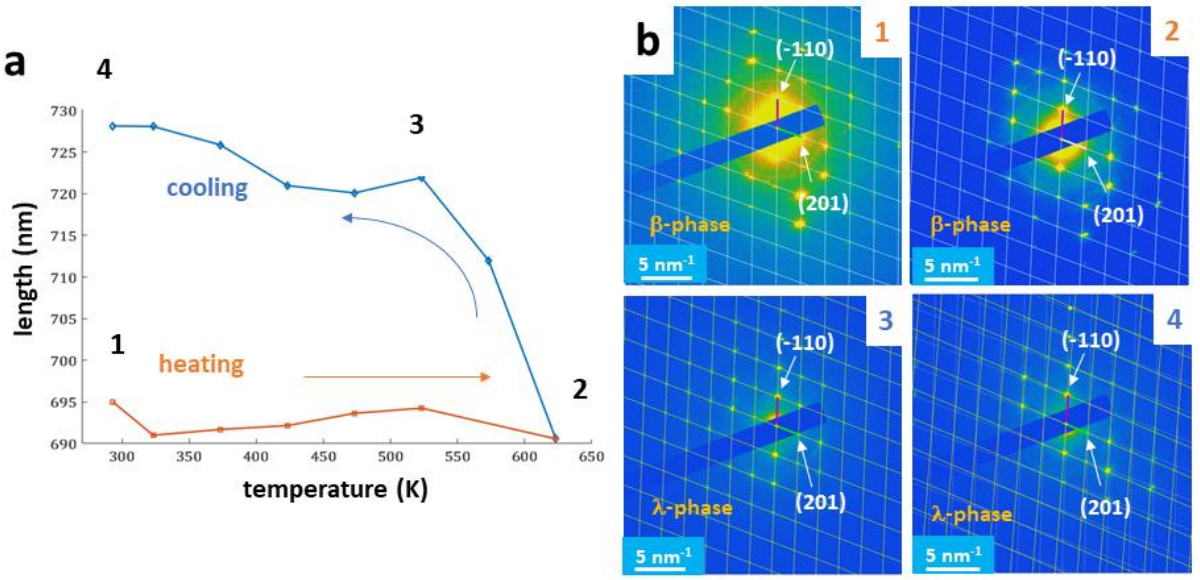

Figure 3. Length measurements of the crystal shown in Figure 2 in the direction of maximum expansion (angle 165° relative to the horizontal). The diffraction patterns at different stages in the heating cycle (points 1 – 4 in the diagram) are shown with best-match indexing. The zone axis is $[11\bar{2}]$.

We have already seen in Figure 1 that the transformation β → α was incomplete and that the single crystal transformed into a larger domain in the λ-phase but with one or several smaller domains remaining in the β-phase although the temperature (625 K) was well above the transition temperature as reported from X-ray studies.[18] Therefore, we have to conclude that a kinetic barrier, that hinders the transformation to the α-phase, exists and is higher in sub-micron crystals than in macroscopic crystals. The observation can be understood on the basis of a high defect density after ball milling. On the other hand, the presence of defects (e.g. dislocations) could change the transformation barrier, e.g., by strain hardening, and hinder the phase transformation by pinning the crystal in the initial phase. At a higher temperature or upon phase changes, an annealing of defects could appear and lower the transformation barrier.

3.2. Switching between the beta and lambda phase under nanosecond laser pulses

To study the response of a Ti_3O_5 crystal to nanosecond laser pulses, a double-tilt room temperature specimen stage was used to align a low-indexed zone axis of the crystals with the electron beam which facilitated the analysis of the diffraction patterns. Experiments at laser wavelengths of 1064 nm allowed the detection of the irreversible transformation β → λ. At 532 nm, the transformation turned out to be more challenging due to the threshold power of the pulses that is needed for the irreversible transformation which was very close to the power that led to a partial amorphization of the material.

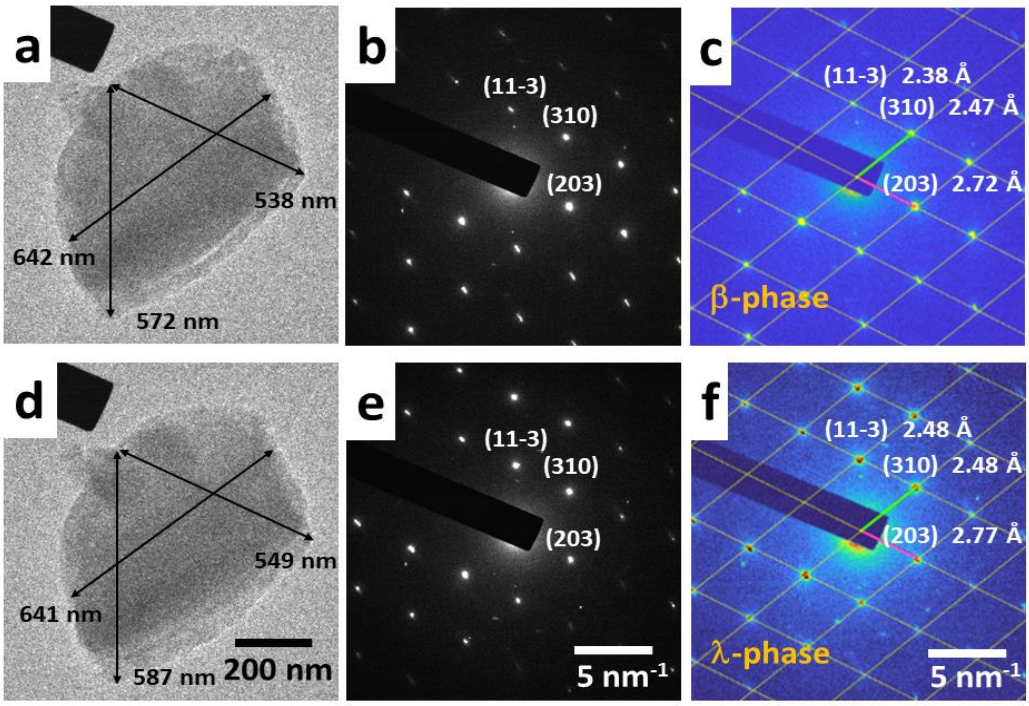

Figure 4. Phase transformation of a Ti_3O_5 crystal under a single laser pulse. Images (a, d), diffraction patterns (b, e) and simulated diffraction patterns (c, f). (a – c): β-phase before the transformation; (d – f): λ-phase after the transformation under a 7 ns laser pulse at 15 mJ/cm^2 and 1064 nm. The measured dimensions of the particle and the spacings of the diffraction spots are indicated. The same directions for the measurements were chosen in diffraction and imaging. In (c) and (f), the experimental patterns are overlaid with the calculated reciprocal lattice of the respective phase in the $[\bar{3}92]$ zone axis (orange lines) which fits the experimental patterns.

Figure 4 shows a Ti_3O_5 crystal before (a – c) and after (d – f) transformation from the β- to the λ-phase under a single laser pulse (7 ns, 15 mJ/cm^2) at 1064 nm. Before recording this series, the crystal has already been exposed to a few laser pulses of lower power that did not result in the phase transformation. Here, a laser power of 15 mJ/cm^2 was necessary to induce the irreversible β → λ transition which can be clearly identified by the changes in the diffraction patterns that match the simulated patterns of the respective phases. The expansion of the crystal upon the transition (appearing as a shrinkage in diffraction) is also measurable in the images of the crystals. A second example is shown in the supporting information (Sect. 3.2).

The measurements are summarized in Table 1. Since a 6.4 % expansion of the monoclinic lattice occurs in the *c*-direction but only 1% in the a- and b-directions,[18] there should be very small size changes in a (hk0)-direction, which is observed indeed in diffraction of the (310)-reflection as well as in imaging. In the other two measured directions (310) and $(11\bar{3})$, the experimental values are

in good agreement with the data from X-ray measurements on polycrystalline samples (in parentheses in Table 1, see Sect. 4 of the supporting information), although the thermal contact between the crystals and the support in X-ray studies, where compressed powder pellets are used, is different from electron microscopy studies of isolated sub-micron crystals. The crystal may slightly move or rotate during the laser pulse, therefore the size measurements in imaging may have small errors due to projection effects. Since the distribution of intensities of the reflections before and after the pulse (Figures 4b, e) doesn't change much, only a small tilt of < 1° may have occurred so that the error in the size measurement must be mainly due to the irregular shape of the crystal. Nevertheless, there is a satisfactory match between the size changes measured in diffraction and imaging.

	beta	**lambda**	**% change**
lattice spacings from diffraction in Å (in parentheses: from X-ray diffraction[27,28])			
(310)	2.47 (2.47)	2.48 (2.47)	±0% (±0%)
(203)	2.72 (2.68)	2.77 (2.72)	+1.8% (+1.5%)
$(11\bar{3})$	2.38 (2.34)	2.48 (2.43)	+4.2% (+3.8%)
size of the particle in nm			
(310)	642	641	±0%
(203)	538	549	+2%
$(11\bar{3})$	572	587	+2.6%

Table 1. Analysis of the diffraction patterns and images shown in Figure 4. The results from electron diffraction are compared with the values from X-ray diffraction (in parentheses) taken from the literature.[27,28]

It is visible that the laser-induced transformation from the β- to the λ-phase is direct and no intermediate coexistence of both phases occurs in one crystal at this laser power. It can also be noticed that some crystallographic defects (seen as double spots or extra spots in diffraction) have vanished during the transformation. It appears that the laser pulses provided enough energy (though within 7 ns) to heat the crystal to sufficiently high temperatures that allowed overcoming the kinetic barrier for the irreversible phase transformation. An associated annealing of defects may also have taken place.

It was previously reported that the transformation from the β- to the λ-phase is observed under laser pulses at 800 nm but not at 400 nm.[6,20] In this study, the transformation at 532 nm seems to occur but is difficult to reproduce because the required laser power is close to the crystal damage limit. However, at 1064 nm, the transformation is reproducible. The duration of the 7 ns laser pulses leads to a more uniform heating of crystals in comparison to the impulsive thermo-

elastic response of a system when sub-picosecond laser pulses were used. The reverse transformation λ → β was not observed with repeated laser pulses, even at higher power. Above pulses with 20-30 mJ cm^{-2} at 1064 nm, the crystal started disintegrating. For a typical crystal with a diameter of 800 nm, the absorption of a 1064 nm pulse is almost 100 %[12], which also seems reasonable in view of the black color of the ball-milled powder used in this study. A temperature rise of a crystal such as in Figure 4 by approximately 100 K at a laser power of 15 mJ/cm^2 can be estimated by taking the specific heat of Ti_3O_5 (710 J kg^{-1} K^{-1}),[3] the density (4500 kg m^{-3}) and an average thickness of the crystals of 400 nm (estimated, c.f., Figure 4). The absorption of Ti_3O_5 is 82 % in a 400 nm layer at 1064 nm.[12] However, an uncertainty remains due to the slightly shifting laser spot with a Gaussian profile, the irregular geometry of the particles and reflection at the surface of the particles. Heating by the electron beam under low-dose conditions is negligible in comparison with laser heating.

4. CONCLUSIONS

The transformation between the different phases in individual sub-micron crystals of Ti_3O_5 is revealed by TEM in imaging and diffraction. It is demonstrated that the expansion of the lattice during the transformation from β to λ, which has hitherto only been seen by diffraction, is associated with a measurable size change of the crystals. Within the measurement error (small in electron diffraction but rather high in imaging), the changes in diffraction and in imaging are in good agreement. In comparison to previous X-ray diffraction studies of macroscopic polycrystalline samples, the phase transitions deviate from the simple picture that resulted from the averaging over many crystallites. The phase transformations of a single nanocrystallite at thermal equilibrium appear to be governed by transition barriers that impede the complete transformations at the nominal transition temperatures. As a result, the transformation from β to λ at 620 K occurs bypassing the α-phase. However, under laser pulses, the transformation from β to λ is complete and seems to benefit from higher temperatures during short time. The present study confirms the high potential of small Ti_3O_5 crystals as photoswitchable materials, where laser pulses are used to switch between the semiconducting and the metallic phase, or when size changes of the material are induced by short laser pulses.

ASSOCIATED CONTENT

Supporting Information

The supporting information contains a detailed description of the experimental setup and the experimental procedure, additional figures, similar measurements as shown in the text above but

on other samples, a consideration and quantitative estimation of radiation effects in the sample, crystallographic data of Ti_3O_5, information about indexing of electron diffraction patterns, and a description of the calculation procedure for the indexing procedure.

ACKNOWLEDGEMENTS

The authors acknowledge financial support from the CNRS-CEA METSA French network (FR CNRS 3507) on the platform IPCMS-UTEM and the Agence Nationale de Recherche, project ANR-22-CE09-0033-01. H. Tokoro and S.-I. Ohkoshi acknowledge support from the JST FOREST Program (JPMJFR213Q), JSPS Grant-in-Aid for Scientific Research (B) (22H02046) and JST Advanced Technologies for Carbon-Neutral (JPMJAN23A2). M. Lorenc gratefully acknowledges the Agence Nationale de la Recherche for financial support under grant ANR-19-CE29-0018 ("Multicross"). Y. Hu thanks the Interdisciplinary Thematic Institute ITI-QMAT in Strasbourg for support.

REFERENCES

(1) De La Torre, A.; Kennes, D. M.; Claassen, M.; Gerber, S.; McIver, J. W.; Sentef, M. A. Nonthermal pathways to ultrafast control in quantum materials. *Rev. Mod. Phys.* **2021**, *93* (4), 041002.

(2) Basov, D. N.; Averitt, R. D.; Hsieh, D. Towards properties on demand in quantum materials. *Nature Mater.* **2017**, *16* (11), 1077-1088.

(3) Tokoro, H.; Yoshikiyo, M.; Imoto, K.; Namai, A.; Nasu, T.; Nakagawa, K.; Ozaki, N.; Hakoe, F.; Tanaka, K.; Chibe, K. et al. External stimulation-controllable heat-storage ceramics. *Nature Comm.* **2015**, *6* (1), 7037.

(4) Ohkoshi, S. I.; Yoshikiyo, M.; MacDougall, J.; Ikeda, Y.; Tokoro, H. Long-term heat-storage materials based on λ-Ti_3O_5 for green transformation (GX). *Chem. Comm.* **2023**, *59* (51), 7875-7886.

(5) Yang, B.; Zhang, Z.; Liu, P.; Fu, X.; Wang, J.; Cao, Y.; Tang, R.; Du, X.; Chen, W.; Li, S. et al. Flatband λ-Ti_3O_5 towards extraordinary solar steam generation. *Nature* **2023**, *622* (7983), 499-506.

(6) Ohkoshi, S. I.; Tsunobuchi, Y.; Matsuda, T.; Hashimoto, K.; Namai, A.; Hakoe, F.; Tokoro, H. Synthesis of a metal oxide with a room-temperature photoreversible phase transition. *Nature Chem.* **2010**, *2* (7), 539-545.

(7) Åsbrink, S.; Magnéli, A. Crystal structure studies on trititanium pentoxide, Ti_3O_5. *Acta Cryst.* **1959**, *12* (8), 575-581.

(8) Hong, S. H.; Åsbrink, S. The structure of γ-Ti_3O_5 at 297 K. *Acta Cryst. B* **1982**, *38* (10), 2570-2576.

(9) Hakoe, F.; Tokoro, H.; Ohkoshi, S. I. Dielectric and optical constants of λ-Ti_3O_5 film measured by spectroscopic ellipsometry. *Mater. Lett.* **2017**, *188*, 8-12.

(10) Ertekin, Z.; Pekmez, N. Ö.; Pekmez, K. One-step electrochemical deposition of thin film titanium suboxide in basic titanyl sulfate solution at room temperature. *J. Solid State Electrochem.* **2020**, *24*, 975-986.

(11) Chen, H.; Hirose, Y.; Nakagawa, K.; Imoto, K.; Ohkoshi, S. I.; Hasegawa, T. Non-metallic electrical transport properties of a metastable λ-Ti_3O_5 thin film epitaxially stabilized on a pseudobrookite seed layer. *Appl. Phys. Lett.* **2020**, *116* (20) 201904.

(12) Yoshimatsu, K.; Kumigashira, H. Direct Synthesis of Metastable λ-Phase Ti_3O_5 Films on $LaAlO_3$ (110) Substrates at High Temperatures. *Crystal Growth Design* **2021**, *22* (1), 703-710.

(13) Araki, Y.; Ohkoshi, S.; Tokoro, H. Synthesis of λ-Ti_3O_5 nanocrystals using a block copolymer. *Mater. Today Energy* **2020**, *18*, 100525.

(14) Cai, Y.; Shi, Q.; Wang, M.; Lv, X.; Cheng, Y.; Huang, W. Synthesis of nanoscale lambda-Ti_3O_5 via a PEG assisted sol-gel method. *J. Alloys Comp.* **2020**, *848*, 156585.

(15) Batdemberel, G.; Ganchimeg, Y.; Enkhtuul, M.; Enkhtsolmon, O.; Munkhsaikhan, G.; Otgonbayar, D. Synthesis and characterization of nanosized Ti_3O_5 crystals under inert gas flow. *Nano Hybrids Comp.* **2022**, *39*, 73.

(16) Asahara, A.; Watanabe, H.; Tokoro, H.; Ohkoshi, S. I.; Suemoto, T. Ultrafast dynamics of photoinduced semiconductor-to-metal transition in the optical switching nano-oxide Ti_3O_5. *Phys. Rev. B* **2014**, *90* (1), 014303.

(17) Ould-Hamouda, A.; Tokoro, H.; Ohkoshi, S. I.; Freysz, E. Single-shot time resolved study of the photo-reversible phase transition induced in flakes of Ti_3O_5 nanoparticles at room temperature. *Chem. Phys. Lett.* **2014**, *608*, 106-112.

(18) Mariette, C.; Lorenc, M.; Cailleau, H.; Collet, E.; Guérin, L.; Volte, A.; Trzop, E.; Bertoni, R.; Dong, X.; Lépine, B. et al. Strain wave pathway to semiconductor-to-metal transition revealed by time-resolved X-ray powder diffraction. *Nature Comm.* **2021**, *12*(1), 1239.

(19) Tasca, K. R.; Esposito, V.; Lantz, G.; Beaud, P.; Kubli, M.; Savoini, M.; Giles, C.; Johnson, S. L. Time-Resolved X-Ray Powder Diffraction Study of Photoinduced Phase Transitions in Ti_3O_5 Nanoparticles. *ChemPhysChem* **2017**, *18* (10), 1385-1392.

(20) Hatanaka, S.; Tsuchiya, T.; Ichikawa, S.; Yamasaki, J.; Sato, K. Ultrafast dynamics of a photoinduced phase transition in single-crystal trititanium pentoxide. *Appl. Phys. Lett.* **2023**, *123* (24), 241902.

(21) Saiki, T.; Yoshida, T.; Akimoto, K.; Indo, D.; Arizono, M.; Okuda, T.; Katsufuji, T. Selection rule for the photoinduced phase transition dominated by anisotropy of strain in Ti_3O_5. *Phys. Rev. B* **2022**, *105* (7), 075134.

(22) Wu, S.; Li, J.; Ling, Y.; Sun, T.; Fan, Y.; Yu, J.; Terasaki, O.; Ma, Y. In Situ Three-Dimensional Electron Diffraction for Probing Structural Transformations of Single Nanocrystals. *Chem. Mater.* **2022**, *34* (18), 8119-8126.

(23) Šepelák, V.; Bégin-Colin, S.; Le Caer, G. Transformations in oxides induced by high-energy ball-milling. *Dalton Trans.* **2012**, *41* (39), 11927-11948.

(24) Rajender, G.; Giri, P. K. Strain induced phase formation, microstructural evolution and bandgap narrowing in strained TiO_2 nanocrystals grown by ball milling. *J. Alloys Comp.* **2016**, *676*, 591-600.

(25) Picher, M.; Bücker, K.; LaGrange, T.; Banhart, F. Imaging and electron energy-loss spectroscopy using single nanosecond electron pulses. *Ultramicroscopy* **2018**, *188*, 41-47.

(26) Hu, Y.; Picher, M.; Tran, N. M.; Palluel, M.; Stoleriu, L.; Daro, N.; Mornet, S.; Enachescu, C.; Freysz, E.; Banhart, F. et al. Photo-thermal switching of individual plasmonically activated spin crossover nanoparticle imaged by ultrafast transmission electron microscopy. *Adv. Mater.* **2021**, *33* (52), 2105586.

(27) Grey, I. E.; Li, C.; Madsen, I. C. Phase equilibria and structural studies on the solid solution $MgTi_2O_5$-Ti_3O_5. *J. Solid State Chem.* **1994**, *113* (1), 62-73.

(28) Kubota, T.; Seiki, R.; Fujisawa, A.; Fadilla, A. F.; Jia, F.; Ohkoshi, S. I.; Tokoro, H. Synthesis of heat storage ceramic λ-Ti_3O_5 using titanium chloride as the starting material. *Mater. Adv.* **2024**, *5* (9), 3832-3837.